OncoTargets and Therapy

Dovepress
open access to scientific and medical research

Open Access Full Text Article

ORIGINAL RESEARCH

Transcatheter arterial embolization combined with radiofrequency ablation activates CD8+ T-cell infiltration surrounding residual tumors in the rabbit VX2 liver tumors

This article was published in the following Dove Press journal:
OncoTargets and Therapy
17 May 2016
Number of times this article has been viewed

Xu-Hua Duan[1,2]
Teng-Fei Li[2]
Guo-Feng Zhou[1,*]
Xin-Wei Han[2,*]
Chuan-Sheng Zheng[1]
Peng-fei Chen[2]
Gan-Sheng Feng[1]

[1]Department of Interventional Radiology, Union Hospital, Tongji Medical College, Huazhong University of Science and Technology, Wuhan, [2]Department of Interventional Radiology, The First Affiliated Hospital, Zhengzhou University, Henan Province, Zhengzhou, People's Republic of China

*These authors contributed equally to this work

Purpose: To evaluate the effect of transcatheter arterial embolization (TAE) combined with radiofrequency ablation (RFA) treatment (TAE + RFA) on the expression of heat shock protein 70 (HSP70) in residual tumors and explore the relationship between the HSP70 and CD8+ T-cell infiltrate surrounding residual tumors in the rabbit VX2 liver tumor model.

Materials and methods: Animals with VX2 liver tumors were randomized into four groups (control, TAE, RFA, and TAE + RFA) with 15 rabbits in each group. Five rabbits in each group were sacrificed on days 1, 3, and 7 after treatment. HSP70 expression and infiltration of CD8+ T-cells in the liver and residual tumors surrounding the necrosis zone were detected by immunohistochemistry staining. The maximal diameters of tumor necrosis, numbers of metastases, and tumor growth rate were compared on day 7 after treatment.

Results: TAE + RFA achieved larger maximal diameter of tumor necrosis, lower tumor growth rate, and fewer metastatic lesions, compared with other treatments on day 7. The number of CD8+ T-cells in the TAE + RFA group was significantly higher than in other groups on days 1, 3, and 7. There was a positive correlation between HSP70 expression level and infiltration of CD8+ T-cells surrounding the residual tumor on day 1 (r=0.9782, P=0.012), day 3 (r=0.93, P=0.021), and day 7 (r=0.8934, P=0.034).

Conclusion: In the rabbit VX2 liver tumor model, TAE + RFA activated the highest number of CD8+ T-cells surrounding residual tumors. TAE + RFA appears to be a beneficial therapeutic modality for tumor control and antitumor immune response in this model.

Keywords: transcatheter arterial embolization, radiofrequency ablation, heat shock protein 70, CD8+ T-cells, liver tumor

Introduction

Hyperthermic ablative therapies using radiofrequency, microwave, laser, or high-intensity focused ultrasonography have become common adjunctive treatments for the local–regional control of unresectable focal malignancies.[1] Radiofrequency ablation (RFA) provides efficacious, cost-effective management of localized cancer sites with survival time comparable to that of surgery in patients with hepatocellular carcinoma nodules.[2,3] Recently, a retrospective study demonstrated that single-session transcatheter arterial embolization (TAE) combined with RFA treatment (TAE + RFA) was an effective and safe treatment in patients with unresectable liver malignancies.[4]

In a previous study, we demonstrated that transcatheter arterial chemoembolization (TACE) combined with RFA (TACE + RFA) and TAE + RFA equally decreased

Correspondence: Guo-Feng Zhou
Department of Interventional Radiology, Union Hospital, Tongji Medical College, Huazhong University of Science and Technology, 1277, Jie-fang Road, Wuhan 430022, People's Republic of China
Tel +86 27 8572 6807
Fax +86 27 8572 6405
Email zzudxh@yeah.net

submit your manuscript | www.dovepress.com
Dovepress
http://dx.doi.org/10.2147/OTT.S95973

tumor growth rate and increased necrotic ratio in the rabbit VX2 liver tumor model, but that TACE + RFA led to more severe liver dysfunction.[5] Hence, we confirmed that TAE + RFA is a beneficial therapeutic modality for treating VX2 liver tumors in this animal model, compared to TACE + RFA, RFA alone, or TACE alone.[5,6] Our data also demonstrated that the tumor growth rate decreased and the necrosis rate increased in the TAE + RFA group on day 7 after treatment, compared to the control, TAE, and RFA groups in the same liver tumor model.[6] In addition, the highest heat shock protein 70 (HSP70) expression was found in residual tumors in the TAE + RFA group, which could activate a strong antitumor immunity response.[6]

Thermal ablative therapy could potentially activate host antitumor immunity and may be of benefit in micrometastatic control and suppression of long-term tumor resistance.[7–9] Increasing evidence indicates that RFA might stimulate antitumor immunity through the induction of HSP70 expression.[10,11] Immunologic and biologic effects have been measured within the tumor lesion by hyperthermia induced by RFA.[12,13] A significant enhancement of the antitumor $CD4^+$ and $CD8^+$ T-cell response was detected after RFA for hepatocellular carcinoma in patients with liver cirrhosis.[12] Chen et al[11] found that hyperthermia induces the release of HSP70 from tumor cells, which activates dendritic cells (DCs) in a paracrine manner, leading to the uptake of tumor antigens chaperoned by HSP70. The subsequent presentation of tumor antigens to native T-cells results in the induction of antigen-specific cytotoxic $CD8^+$ T-cells. In our previous study, different levels of HSP70 expression were found in the residual tumors of rabbits following treatment with TAE, RFA, or TAE + RFA.[6] In the previous study, residual liver tumor animal models were generated by TAE + RFA, RFA, and TAE in rabbit VX2 liver tumors.[6] The aim of the present study was to further characterize the effect of these treatments on the expression of HSP70 and the activating $CD8^+$ T-cells in the liver and residual tumors surrounding the necrosis zone in the rabbit VX2 liver model. Furthermore, it was explored if TAE + RFA treatment could have a stronger ability to activate $CD8^+$ T-cells than other ablative treatments.

Materials and methods

Animals and rabbit VX2 liver tumor models

Animal experiments were approved by the Animal Care Committee of Hubei Province, People's Republic of China. Adult Japanese white rabbits weighing 2.5–3.0 kg (4–5 months old, regardless of sex) were used. All experiments were performed according to the guidelines for animal care of the Hubei Province Animal Experiments Committee. Animals were housed in the local animal facility in single cages for rabbits with food and drinking water adlibitum. The VX2 carcinoma strain was maintained by successive transplantation into the hind limb of carrier rabbits by deep intramuscular injection.[5] Two weeks after inoculation, surgical implantation of a freshly harvested VX2 tumor fragment measuring 1 mm^3 was embedded 10 mm deep into the medial left liver lobe to generate liver tumors. To localize and measure the size of the VX2 tumor, magnetic resonance imaging (MRI) was performed with a 1.5 T MRI (Magnetom Avanto; Siemens Medical Solutions, Erlangen, Germany) 15 days after inoculation. Subsequent procedures were performed when the tumors reached ~1.5 cm in diameter, as measured by MRI. Tumors were successfully established in all 60 rabbit livers implanted. Animals were randomized into four groups (control, TAE, RFA, and TAE + RFA groups) with 15 rabbits in each group. One day before the experimental procedure, the epigastria and backs of all rabbits were shaved. Following each procedure, the animals were monitored until they recovered from anesthesia in their cages.

Control, TAE, and RFA procedures

Rabbits in the control group were subjected to no procedure until sample collection. TAE procedures were performed under digital subtraction angiography guidance. After celiac arteriography with a 4F Cobra C2 catheter (Terumo, Tokyo, Japan), a 2.7F (Terumo) coaxial catheter system was advanced into the left hepatic artery. After a manual bolus injection of contrast medium to confirm location of the tumor, 0.1–0.4 mL of 150–250 μm polyvinyl alcohol particles (Cook, Bloomington, IN, USA) mixed with contrast media was carefully injected (manually) through the catheter to embolize the tumor feeding artery, as previously described.[5] The embolization endpoint was complete stasis of antegrade blood flow. The RFA procedure was performed with the RITA 1500 system (RITA Medical Systems, Mountain View, CA, USA) and 14-gauge starburst multiarray electrodes, as previously described.[6] For the TAE + RFA group, RFA was performed 15 minutes after TAE.

Sample collection

After procedures, all animals were monitored until they recovered from anesthesia and then placed in cages. Five rabbits from each group were sacrificed on days 1, 3, and 7 after the procedures. Blood samples were collected from all rabbits 1 day before the procedures and 3 and 7 days after the procedures. Plasma levels of alanine aminotransferase (ALT) and

aspartate aminotransferase (AST) were measured using standard enzymatic procedures. The whole liver was harvested after the death of each animal. The sample collection methods in the four groups were as previously described.[6]

Evaluation of diameters of tumor necrosis and tumor growth

Seven days after the procedure, intrahepatic and extrahepatic metastases were counted by gross inspection and pathology of the liver, lung, and peritoneum. The tumor was cut along the long axis for the evaluation of diameters of tumor necrosis and tumor growth. The tumor volume was calculated according to the following formula: $a \times b^2/2$, where "a" and "b" represented the maximum and minimum diameters of the tumor, respectively. The tumor growth rate was evaluated by the ratio of tumor volume before and after therapy. The tumor was longitudinally sectioned at 3–5 mm intervals and the largest slice in the middle was preserved in 4% paraformaldehyde for pathological analysis.

Immunohistochemistry staining of HSP70 and CD8+ T-cells

Each tissue sample was embedded in paraffin and sectioned at 4 μm. Two specimens were deparaffinized at 65°C for 2 hours and washed in phosphate-buffered saline (pH 7.4). The specimens were heated in boiling Tris-ethylenediaminetetraacetic acid (0.01 M, pH 6.0) for 10 minutes in a microwave oven, and endogenous peroxidase was blocked with methanol containing 3% hydrogen peroxide for 10 minutes and cooled to room temperature. For immunohistochemical detection of HSP70 and CD8+ T-cells, one specimen was incubated overnight at 4°C with mouse anti-HSP70 (1:100 dilution; Abcam PLC, Cambridge, UK), while another was incubated overnight at 4°C with mouse anti-CD8+ (1:100 dilution; Santa Cruz Biotechnology Inc., Dallas, TX, USA). The sections were then incubated with an anti-mouse secondary antibody (REAL™ EnVision+/horseradish peroxidase rabbit/mouse; Dako Denmark A/S, Glostrup, Denmark) for 45 minutes at room temperature. Binding reactions were visualized by 3-3′-diaminobenzidine tetrahydrochloride substrate to detect the positive cells with HSP70 and CD8+ expression. Negative controls were run by replacing the primary antibody with phosphate-buffered saline.

Imaging analysis

Image-Pro Plus software (Version 6.0; Media Cybernetics, Bethesda, MD, USA) was used for imaging analysis. After immunohistochemistry staining, all the HSP70 slides were examined by two experienced pathologists in a blinded manner. Measurement of integrated optical density (IOD) of HSP70 expression in each group at different time points was performed as previously described.[6]

The number of CD8+ T-cells was also counted using Image-Pro Plus software. In the control group, photographs were taken from the border regions of the tumor and normal liver tissue. In the TAE, RFA, and TAE + RFA groups, photographs were taken from the residual tumor and the normal liver tissue surrounding the necrosis zone. Five independent microscopic fields (×200 magnification), representing the densest lymphocytic infiltrates, were selected for each rabbit to ensure representativeness and homogeneity.

Statistical analysis

Statistical analysis was performed using Statistical Package for the Social Sciences Version 13.0 (SPSS Inc., Chicago, IL, USA). Data were expressed as mean ± standard deviation. One-way analysis of variance was used to compare the maximum diameter of tumor necrosis and the tumor growth rates in different groups on day 7. Mann–Whitney *U*-test was used to compare ALT and AST levels between the two groups at different time points. Mann–Whitney *U*-test was also used to compare the HSP70 and CD8+ T-cells between the two groups at the same time point and between two time points within the same group. Spearman's rank correlation coefficient was used to assess correlation between variables. A *P*-value of <0.05 was considered statistically significant.

Results

Fifteen days after tumor implantation, the maximum diameter of tumors for the 60 rabbits ranged from 11.8 to 17.4 mm (mean ± standard deviation: 14.8±3.8 mm). All the rabbits tolerated the surgical procedures, recovered uneventfully, and survived to the end of the study.

Comparison liver function changes in different groups pre- and postprocedure

Figure 1 shows that the ALT and AST levels in the TAE + RFA group were not significantly different from the other groups on the day before the operation ($P>0.05$). The ALT and AST levels in the TAE + RFA, RFA, and TAE groups peaked on day 3 and decreased by day 7. The TAE + RFA group showed the highest ALT and AST levels on day 3 (all $P<0.05$). On day 3, the ALT and AST levels in RFA groups were significantly greater than in the TAE and control groups ($P<0.05$). On day 7, there was no significant difference in the ALT and AST levels between the TAE + RFA and RFA groups. On day 7, the ALT and AST levels in TAE + RFA and RFA groups were significantly greater than in the TAE

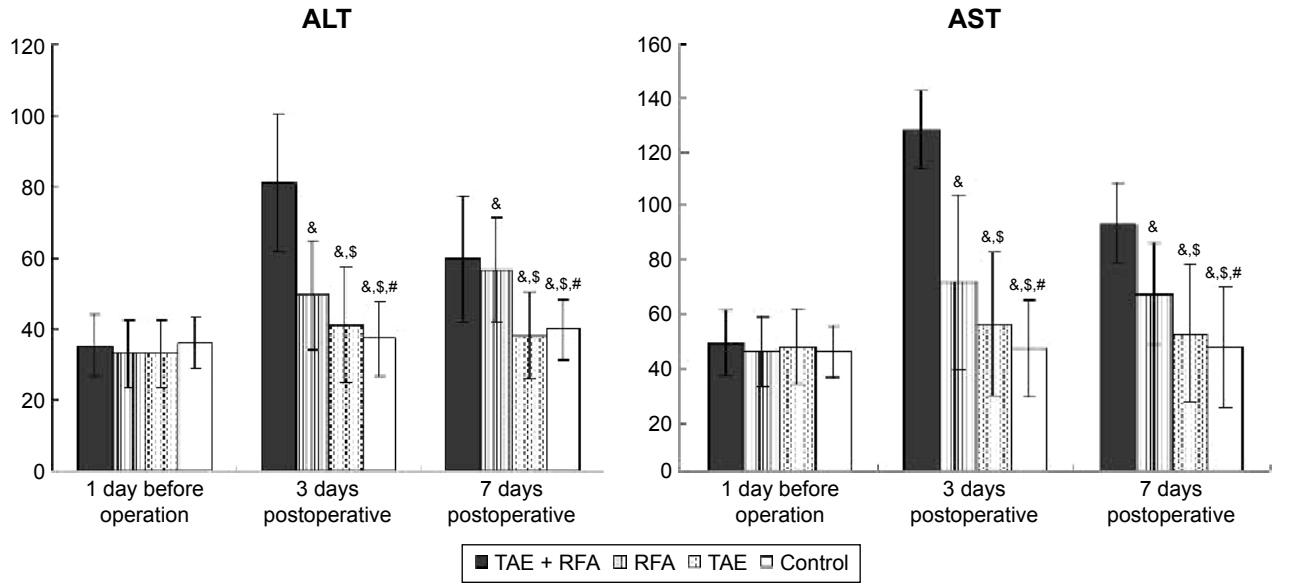

Figure 1 Changes in serum ALT (U/L) and AST (U/L) levels before and after treatment.
Notes: [&]$P<0.05$: ALT and AST levels in the TAE + RFA group were significantly higher compared to the other groups on day 3 after the operation. [$]$P<0.05$: ALT and AST levels in the RFA group were significantly higher than in TAE and control groups on day 3. [#]$P>0.05$: There was no significant difference in ALT and AST levels between the TAE and Control group on day 3 and 7. Results are in response to Mann–Whitney *U*-test.
Abbreviations: ALT, alanine aminotransferase; AST, aspartate aminotransferase; RFA, radiofrequency ablation; TAE, transcatheter arterial embolization; TAE + RFA, transcatheter arterial embolization combined with radiofrequency ablation.

and control groups ($P<0.05$). The ALT and AST levels in the TAE + RFA group were not significantly different from the RFA group on day 7 ($P>0.05$).

Effect of different treatments on the number of metastases, maximum diameters of tumor necrosis, and tumor growth rate on day 7

The mean maximum long- and short-axis diameters of the gross specimens were measured in different groups on day 7 (Table 1). The mean maximum long- and short-axis diameters of tumor necrosis rate and tumor growth rate between the TAE + RFA group and the other groups differed significantly ($P<0.05$). Seven days after treatment, the tumor growth rate was significantly decreased, whereas the number of intrahepatic and extrahepatic metastases in the TAE + RFA group was the lowest compared to that in other groups (Table 2).

IOD of HSP70 expression in liver surrounding the necrosis zone

There was no evidence of HSP70 expression in the control group at any of the three time points. Occasionally hepatocytes exhibited HSP70 expression in the TAE group at the three time points. HSP70 expression surrounding the coagulated tissue margins significantly increased on day 1 in the RFA and TAE + RFA groups. The peak response in liver occurred on day 3 in the RFA and TAE + RFA groups (Figure 2).

Table 1 Comparison of maximal diameter of tumor necrosis in different groups on day 7

Group (n)	Long diameter (mm)	Short diameter (mm)
TAE + RFA (5)	14.4±1.4	8.9±1.4
RFA (5)	12.7±2.9[&]	6.4±1.3[&]
TAE (5)*	7.9±1.5[&,$]	4.1±0.6[&,$]
Control (5)	3.9±1.3[&,$,#]	2.1±0.7[&,$,#]

Notes: *Diameters of infarcted zones by TAE group. Results are in response to one way analysis of variance. [&]$P<0.05$: TAE + RFA group compared with the other groups. [$]$P<0.05$: RFA group compared with TAE and control groups. [#]$P<0.05$: TAE group compared with the control group.
Abbreviations: RFA, radiofrequency ablation; TAE, transcatheter arterial embolization; TAE + RFA, transcatheter arterial embolization combined with radiofrequency ablation.

Table 2 Tumor growth rate and number of metastases in different groups on day 7

Group (n)	Tumor growth rate (%)	Number of metastases (n)
TAE + RFA (5)	118.97±43.11	0.6±0.5
RFA (5)	269.15±39.94[&]	4.8±1.9[&]
TAE (5)	369.48±48.31[&,$]	10.4±3.4[&,$]
Control (5)	425.48±51.31[&,$,#]	16.9±4.6[&,$,#]

Notes: Results are in response to one way analysis of variance. [&]$P<0.01$: TAE + RFA group compared with the other groups. [$]$P<0.05$: RFA group compared with TAE and control groups. [#]$P<0.05$: TAE group compared with the control group.
Abbreviations: RFA, radiofrequency ablation; TAE, transcatheter arterial embolization; TAE + RFA, transcatheter arterial embolization combined with radiofrequency ablation.

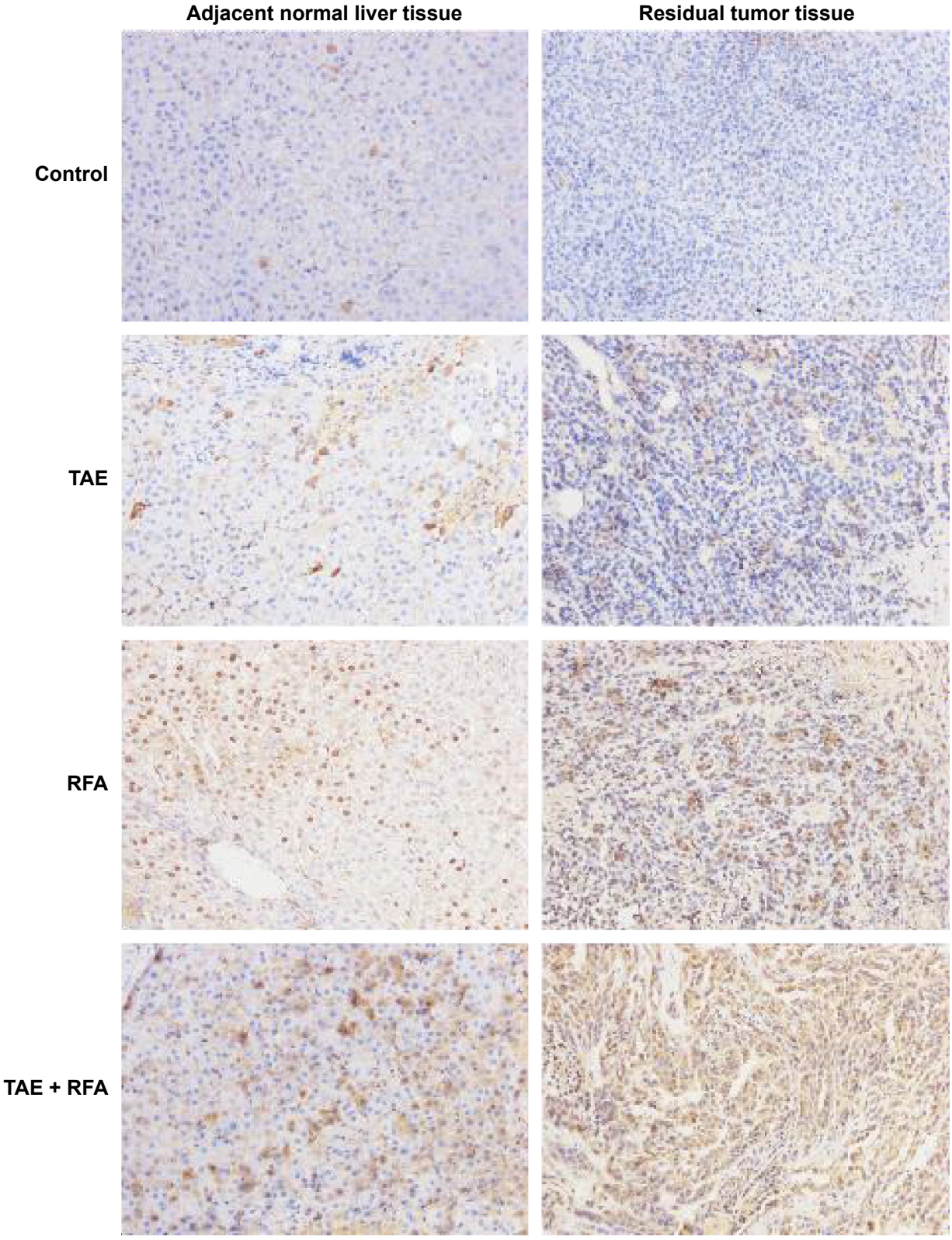

Figure 2 Representative immunohistochemical analysis (×200 magnification) showing peak HSP70 expression in adjacent normal liver surrounding the liver necrosis zone and residual tumors on day 3.

Notes: No expression in adjacent normal liver tissue and little HSP70 expression were seen in tumor tissue in the control group. Some positive HSP70 staining cells in liver tissue and increased HSP70 expression were observed in residual tumors in the TAE group. In the RFA group, apparent HSP70 expression in liver tissue and stronger HSP70 expression in residual tumors were observed. Prominent HSP70 expression in liver tissue and the highest HSP70 expression in residual tumors were seen in TAE + RFA group.

Abbreviations: HSP70, heat shock protein 70; RFA, radiofrequency ablation; TAE, transcatheter arterial embolization; TAE + RFA, transcatheter arterial embolization combined with radiofrequency ablation.

Figure 3 shows the IOD of HSP70 expression measured in the liver surrounding the necrosis zone in different groups at different time points. The TAE + RFA group had a significantly higher IOD than the other groups on days 1, 3, and 7. In the TAE + RFA group, HSP70 expression on day 3 was significantly higher than on day 1 (3,776.98±991.22 versus 2,142.32±330.61, P=0.002) and day 7 (3,776.98±991.22 versus 2,158.29±412.25, P=0.001). HSP70 in the RFA group was significantly higher than in the controls on days 1, 3, and 7. In the RFA group, HSP70 on day 3 was significantly increased compared to the levels observed on day 1 (2,704.89±875.20 versus 976.32±341.16, P=0.008) and day 7 (2,704.89±875.20 versus 1,625.66±210.32, P<0.001).

IOD of HSP70 expression in residual tumors surrounding the tumor necrosis zone

In the RFA and TAE + RFA groups, HSP70 expression in residual tumor cells showed obvious staining in on day 1, which peaked on day 3, and dropped on day 7 (Figure 4). There was no significant evidence of HSP70 expression in the control group on any of the three observation time points.

The IOD of HSP70 expression measured in the residual tumor surrounding the necrosis zone in different groups at different time points is compared in Figure 4. The IOD of HSP70 expression TAE + RFA group was significantly higher than the other groups on days 1, 3, and 7. In the TAE + RFA group, HSP70 expression was significantly higher on day 3 than on day 1 (31,967.67±6,708.48 versus 16,802.12±3,411.19, P<0.001) and day 7 (31,967.67±6,708.48 versus 23,199.83±2,986.49, P=0.004). The IOD of the RFA group was higher than that of the controls on days 1, 3, and 7. In the RFA group, HSP70 was significantly higher on day 3 than on day 1 (11,149.78±2,228.96 versus 7,113.22±2,404.15, P=0.005) and day 7 (11,149.78±2,228.96 versus 6,963.66±1,845.79, P=0.003).

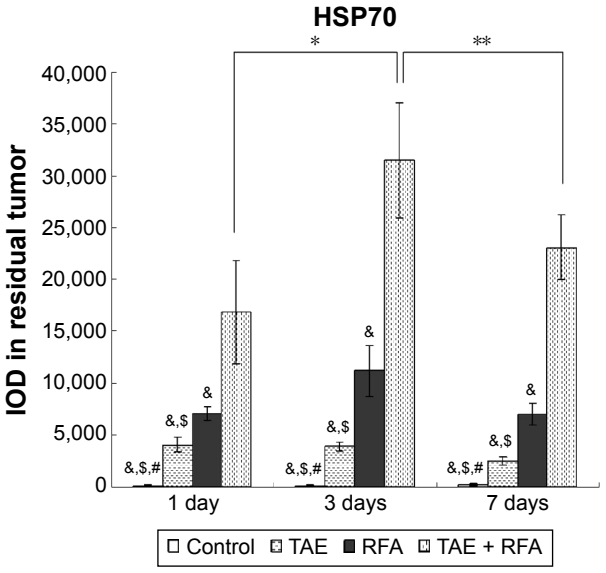

Figure 4 IOD of HSP70 expression measured in the residual tumor surrounding the tumor necrosis zone.

Notes: The IOD of the TAE + RFA group was significantly higher than that of other groups (n=5, $^{\&}P$<0.01) on days 1, 3, and 7. The RFA group had a significantly higher HSP70 expression compared with the TAE and control groups (n=5, $^{\$}P$<0.05) on days 1, 3, and 7. The TAE group was significantly higher than the control group (n=5, $^{\#}P$<0.05) on days 1, 3, and 7. In the TAE + RFA group, the IOD on day 3 was higher than on day 1 (n=5, *P<0.05) and day 7 (n=5, **P<0.05). Results are in response to Mann–Whitney U-test.

Abbreviations: HSP70, heat shock protein 70; IOD, integrated optical density; RFA, radiofrequency ablation; TAE, transcatheter arterial embolization; TAE + RFA, transcatheter arterial embolization combined with radiofrequency ablation.

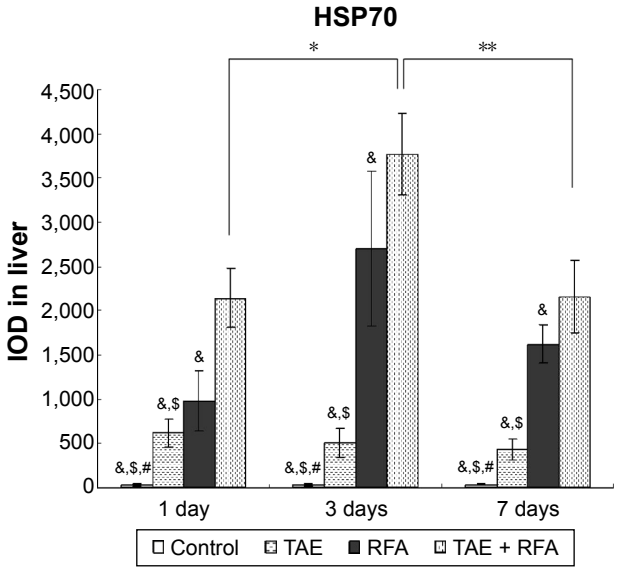

Figure 3 IOD of HSP70 expression surrounding the liver necrosis zone.

Notes: The IOD of the TAE + RFA group was significantly higher than that of other groups (n=5, $^{\&}P$<0.01) on days 1, 3, and 7. The RFA group had significantly higher HSP70 expression compared with the TAE and control groups (n=5, $^{\$}P$<0.05) on days 1, 3, and 7. The IOD of the TAE group was statistically significantly higher than that of the control group (n=5, $^{\#}P$<0.05) on days 1, 3, and 7. In the TAE + RFA group, the IOD on day 3 was higher than on day 1 (n=5, *P<0.05) and day 7 (n=5, **P<0.05). Results are in response to Mann–Whitney U-test.

Abbreviations: HSP70, heat shock protein 70; IOD, integrated optical density; RFA, radiofrequency ablation; TAE, transcatheter arterial embolization; TAE + RFA, transcatheter arterial embolization combined with radiofrequency ablation.

Correlation of HSP70 levels and infiltration of CD8$^+$ T-cells surrounding the liver and the residual tumor

There was no significant difference in the number of CD8$^+$ T-cells surrounding the liver necrosis zone in the four groups at different time points (Table 3). The HSP70 levels in liver were not significantly correlated with CD8$^+$ T-cell infiltration on days 1, 3, and 7 in any of the groups.

Faint infiltrate of CD8$^+$ T-cells in the portal area was observed in the liver transitional zone and surrounding the

Table 3 The number of CD8+ T-cells infiltrated in the liver surrounding the liver necrosis zone in different groups at different time points

Group (n)	1 day	3 days	7 days
TAE + RFA (5)	6.9±2.1	7.9±2.4	10.7±3.8
RFA (5)	7.1±1. 2	5.7±3.1	7.3±2.1
TAE (5)	5.5±1. 8	5.5±4.0	7.3±1.6
Control (5)	2.4±0.8	2.9±0.1	6.2±1.5

Notes: There was no significant difference in the four groups on days 1, 3, and 7. Results are in response to Mann–Whitney *U*-test.
Abbreviations: RFA, radiofrequency ablation; TAE, transcatheter arterial embolization; TAE + RFA, transcatheter arterial embolization combined with radiofrequency ablation.

residual tumors in the control group on three occasions. In the TAE, RFA, and TAE + RFA groups, the number of CD8+ T-cells infiltrated in the transitional zone and surrounding the residual tumor was higher on days 1 and 3 and peaked on day 7 (Figure 5). On day 7, significant infiltration of CD8+ T-cells was seen not only at the margin, but also in the center of residual tumors in the TAE + RFA group. However, in the RFA group, we only found infiltration of CD8+ T-cells at the margins (Figure 5).

The number of infiltrating CD8+ T-cells surrounding the residual tumors at different time points is shown in Table 4. In the TAE + RFA group, significantly more CD8+ T-cells were observed compared to the other groups on days 1, 3, and 7. In the TAE + RFA group, the number of CD8+ T-cells was higher on day 7 than on day 1 (73.73±6.79 versus 32.4±6.22, $P<0.001$) and day 3 (73.73±6.79 versus 47.9±10.42, $P<0.001$). In the RFA group, more CD8+ T-cells were seen on day 7 compared to day 1 (44.83±6.17 versus 17.27±5.12, $P<0.001$) and day 3 (44.83±6.17 versus 29.67±4.78, $P<0.001$). The CD8+ T-cells in the TAE group were significantly higher than the control group on days 1, 3, and 7 (all $P<0.05$).

In the control, TAE, RFA, and TAE + RFA groups, HSP70 expression in residual tumor cells showed a significant positive correlation with infiltration of CD8+ T-cells in the vicinity of the residual tumors on day 1 ($r=0.9782$, $P=0.012$), day 3 ($r=0.93$, $P=0.021$), and day 7 ($r=0.8934$, $P=0.034$).

Discussion

Localized hyperthermia induced by thermal ablation has been reported to enhance the immunogenicity of cancer cells concomitantly with the expression of HSPs.[7–9] HSPs derived from tumor cells can serve as cytokines that can stimulate DCs and macrophages to produce proinflammatory cytokines and chemokines.[14,15] More importantly, HSPs are capable of chaperoning tumor antigens to DCs and monocytes/macrophages and then cross-presenting the antigens to T-cells, and thus, induce antitumor immunity.[11,16] HSP70 is the major HSP responsible for the autocrine induction of chemokines by tumor cells.[11]

Induced HSP70 can bind to the antigenic peptides of the tumor cells and deliver them to macrophages and other antigen-presenting cells both in vitro and in vivo.[17,18] Liu et al[19] evaluated the effect of combining RFA with heat-shocked tumor cell lysate-pulsed DC vaccination on the poorly immunogenic B16F10-luc melanoma. They found that this combined treatment induces strong and durable T-cell–mediated tumor-specific immunity that results in the efficient destruction of remnant tumor cells and prevents tumor recurrence following RFA. This immunity was mediated mainly by CD8+ T-cells.[19]

Wissniowski et al[20] found a marked increase of CD3+ T-cells not only at the margin between thermically altered normal liver and tumor, but also within the center of the tumor 2 weeks after RFA. Pulmonary metastases were reported to spontaneously regress following RFA in renal cell carcinoma.[21,22] RFA may be involved in stimulating the host immune system, similar to the effect of immunotherapy using interferon.[22] In addition, Schueller et al[8] observed an increased cytotoxic T-lymphocyte response against human hepatocellular carcinoma after hyperthermia.

In the present study, we found a marked increase of CD8+ T-cell infiltrate surrounding the residual tumors in the RFA group and especially in the TAE + RFA group on day 7. This phenomenon is consistent with the Wissniowski et al[20] study, although we measured CD8+ T-cells instead of CD3+ T-cells. These inflammatory infiltrates are suspected to be the area in which tumor antigens are presented to CD8+ T-cells.

The surviving tumor and tissue cells undergo heat shock, leading to increased HSP70 expression, which may form complexes with antigenic peptides, enhance their antigenicity, and direct them to major histocompatibility complex class I and II pathways for presentation to T-cells.[8,23,24] In our study, apparent HSP70 expression was found in liver in the TAE, RFA, and TAE + RFA groups on days 1, 3, and 7. However, there was no significant difference in the number of CD8+ T-cell infiltrates surrounding the liver necrosis zone in these groups on any of the days. The HSP70 levels in liver did not show a significantly positive correlation with the number of CD8+ T-cells on any day or in any group. Our data agree with Srivastava[16] that it is not HSP70 expressed in normal tissue, but tumor-derived HSP70 as a potent adjuvant that can facilitate the presentation of tumor antigens and induces antitumor immunity.

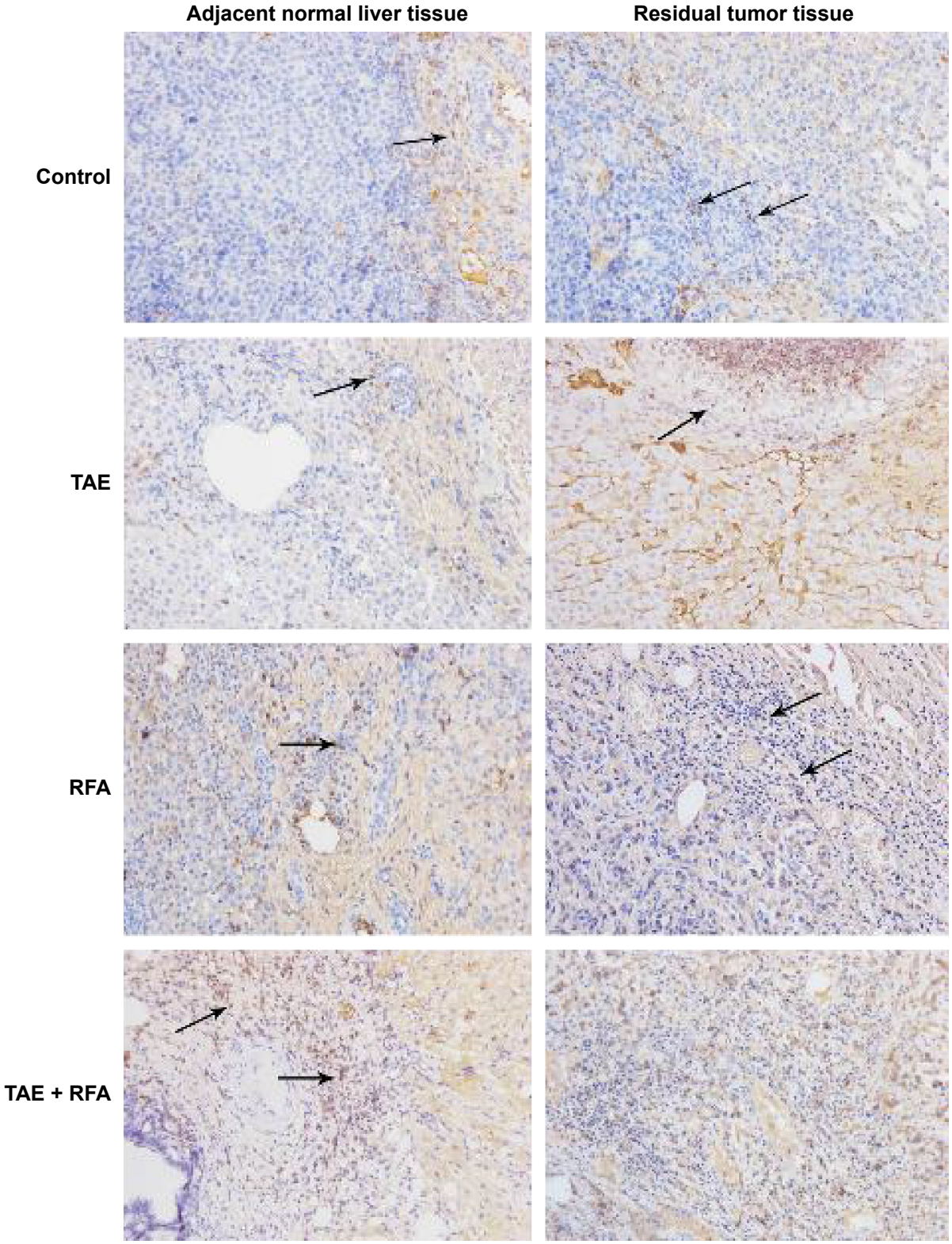

Figure 5 Representative photomicrographs of immunostaining (×200 magnification) showing infiltration of $CD8^+$ T-cells in the liver transitional zone and surrounding the residual tumors on day 7.

Notes: In the control group, faint $CD8^+$ T-cell infiltrate (arrow) in the portal area was observed in the liver transitional zone and surrounding the residual tumors (arrows). In the TAE group, some $CD8^+$ T-cells in the portal area (arrow) were seen in the transitional zone and surrounding the residual tumors (arrow). In the RFA group, an increase in $CD8^+$ T-cell infiltrate in the portal area was seen in the transitional zone (arrow) and surrounding the residual tumors (arrows). In the TAE + RFA group, a marked increase of $CD8^+$ T-cell infiltrate in the portal area was observed in the transitional zone (arrows). The most significant infiltration of $CD8^+$ T-cells was observed at the margin and in the center of the residual tumors.

Abbreviations: RFA, radiofrequency ablation; TAE, transcatheter arterial embolization; TAE + RFA, transcatheter arterial embolization combined with radiofrequency ablation.

Table 4 The number of infiltrating CD8+ T-cells surrounding residual tumors at different time points

Group (n)	1 day	3 days	7 days
TAE + RFA (5)	32.4±6.22**	47.9±10.42*	73.73±6.79
RFA (5)	17.27±5.12&,**	29.67±4.78&,*	44.83±6.17&
TAE (5)	10.56±3.58&,$,**	15.53±4.56&,$,*	26.53±7.56&,$
Control (5)	2.43±0.85&,$,#	2.57±0.81&,$,#	6.17±1.79&,$,#

Notes: The number of CD8+ T-cells in the TAE + RFA group was significantly higher than the number observed in other groups (&$P<0.01$) on days 1, 3, and 7. The RFA group had significantly higher HSP70 expression compared with the TAE and control groups ($^{\$}P<0.05$) on days 1, 3, and 7. The TAE group was statistically significantly higher than the control group ($^{\#}P<0.05$) on days 1, 3, and 7. In the TAE + RFA, RFA, and TAE groups, more CD8+ cells were observed on day 7 compared to day 3 ($^{*}P<0.05$) and day 1 ($^{**}P<0.05$). Results are in response to Mann–Whitney *U*-test.

Abbreviations: HSP70, heat shock protein 70; RFA, radiofrequency ablation; TAE, transcatheter arterial embolization; TAE + RFA, transcatheter arterial embolization combined with radiofrequency ablation.

Faint CD8+ T-cell infiltrate was observed in the zone surrounding the tumor at the three observed time points. However, the rabbits in the TAE, RFA, and RFA + TAE groups raised a significant CD8+ T-cell response surrounding the residual tumors. We found the most significant infiltration of CD8+ T-cells around the residual tumors on day 7, when HSP70 showed peak expression in the TAE + RFA group. Our data confirmed the positive correlation between the expression of HSP70 and the infiltration of CD8+ T-cells in the vicinity of the residual tumors.

Although TAE + RFA led to more severe liver dysfunction compared with RFA on day 3, there was no significant difference in ALT and AST levels between TAE + RFA and RFA treatment on days 1, 3, and 7. TAE + RFA can achieve the same survival time with temporary liver dysfunction comparable to RFA in treating rabbit VX2 liver tumors. So, it was better for us to prolong the observation time to evaluate the effect on tumor control and antitumor immune response in this animal model. Meanwhile, the TAE + RFA combination was more effective in achieving maximal diameters of tumor necrosis, lower tumor growth, and fewer metastases, compared to the other treatments. Two possible mechanisms could describe the potential relationship between TAE + RFA treatment and the destruction of tumor tissue. First, there may be a synergistic effect of hypoxia and hyperpyrexia generated by the TAE combined with RFA, as we previously reported.[6] Alternately, TAE + RFA might activate the highest number of CD8+ T-cells surrounding the residual tumor, which may reflect an antitumor immune response. In the present study, HSP70 expression was increased on day 1, peaked on day 3, and dropped on day 7 in the RFA and TAE + RFA groups. Heat stress upregulates HSP70, which then binds tumor antigens and mediates their uptake into antigen-presenting cells, resulting in the induction of antigen-specific cytotoxic CD8+ T-cells. Chen et al[11] found that 24 hours after hyperthermia, DCs in the spleen and lymph nodes increased and the induction of tumor antigen-specific cytotoxic T-lymphocyte was improved. In our study, infiltration of CD8+ T-cells surrounding the residual tumors was enhanced on day 3 and peaked on day 7. Hence, these immune responses would likely continue with the high expression of HSP70 surrounding the residual tumors, if we prolong the observation time. Next, comprehensive evaluation of antitumor immune response and its efficacy on tumor control could be monitored in this animal model.

The present study had several limitations. Due to the lack of antibody reagents for the rabbit VX2 liver tumors, which is the major model for local ablative treatments, it was not possible to conduct in-depth histopathological and immunohistochemical examination. Due to space constraints, we only showed the most representative immunohistochemical changes in different groups, which were the peak of HSP70 expression on day 3 and CD8+ T-cell infiltration on day 7. Moreover, monitoring the number of CD8+ T-cells is not absolute proof that antitumor immunity was enhanced. Additional studies are needed to monitor CD4+, natural killer and natural killer T-cells, macrophages and DCs, and regulatory T-cells in residual tumors, in order to observe how effectively different levels of HSP70 expression induce antitumor immune responses.

Conclusion

Our data show that TAE + RFA activates the highest number of CD8+ T-cells surrounding residual tumors compared to other methods, by inducing HSP70 expression in residual tumor cells in rabbit VX2 liver tumor model. Treating rabbit VX2 liver tumors with TAE + RFA appears to be a robust experimental model for observing how different levels of HSP70 expression in residual tumors effectively induce antitumor immune responses. HSP70 may represent a promising therapeutic target for adjuvant immune therapy.

Acknowledgment

This work was supported by a grant from the National Natural Science Foundation of China (No 81401494). Neither the entire paper nor any part of its content has been published or has been accepted elsewhere.

Author contributions

All authors contributed toward data analysis, drafting and revising the paper and agree to be accountable for all aspects of the work.

Disclosure

The authors report no conflicts of interest in this work.

References

1. Bhardwaj N, Strickland AD, Ahmad F, Dennison AR, Lloyd DM. Liver ablation techniques: a review. *Surg Endosc*. 2010;24(2):254–265.
2. Liu CH, Arellano RS, Uppot RN, Samir AE, Gervais DA, Mueller PR. Radiofrequency ablation of hepatic tumours: effect of post-ablation margin on local tumour progression. *Eur Radiol*. 2010;20(4):877–885.
3. Lu DS, Yu NC, Raman SS, et al. Radiofrequency ablation of hepatocellular carcinoma: treatment success as defined by histologic examination of the explanted liver. *Radiology*. 2005;234(3):954–960.
4. Bonomo G, Della Vigna P, Monfardini L, et al. Combined therapies for the treatment of technically unresectable liver malignancies: bland embolization and radiofrequency thermal ablation within the same session. *Cardiovasc Intervent Radiol*. 2012;35(6):1372–1379.
5. Duan X, Zhou G, Han X, et al. Radiofrequency ablation combined with transcatheter therapy in rabbit VX2 liver tumors: effects and histopathological characteristics. *Acta Radiol*. 2015;56(1):87–96.
6. Duan X, Zhou G, Zheng C, et al. Heat shock protein 70 expression and effect of combined transcatheter arterial embolization and radiofrequency ablation in the rabbit VX2 liver tumour model. *Clin Radiol*. 2014;69(2):186–193.
7. Hansler J, Wissniowski TT, Schuppan D, et al. Activation and dramatically increased cytolytic activity of tumor specific T lymphocytes after radio-frequency ablation in patients with hepatocellular carcinoma and colorectal liver metastases. *World J Gastroenterol*. 2006;12(23):3716–3721.
8. Schueller G, Kettenbach J, Sedivy R, et al. Heat shock protein expression induced by percutaneous radiofrequency ablation of hepatocellular carcinoma in vivo. *Int J Oncol*. 2004;24(3):609–613.
9. Todorova VK, Klimberg VS, Hennings L, Kieber-Emmons T, Pashov A. Immunomodulatory effects of radiofrequency ablation in a breast cancer model. *Immunol Invest*. 2010;39(1):74–92.
10. Yang WL, Nair DG, Makizumi R, et al. Heat shock protein 70 is induced in mouse human colon tumor xenografts after sublethal radiofrequency ablation. *Ann Surg Oncol*. 2004;11(4):399–406.
11. Chen T, Guo J, Han C, Yang M, Cao X. Heat shock protein 70, released from heat-stressed tumor cells, initiates antitumor immunity by inducing tumor cell chemokine production and activating dendritic cells via TLR4 pathway. *J Immunol*. 2009;182(3):1449–1459.
12. Zerbini A, Pilli M, Penna A, et al. Radiofrequency thermal ablation of hepatocellular carcinoma liver nodules can activate and enhance tumor-specific T-cell responses. *Cancer Res*. 2006;66(2):1139–1146.
13. Zerbini A, Pilli M, Fagnoni F, et al. Increased immunostimulatory activity conferred to antigen-presenting cells by exposure to antigen extract from hepatocellular carcinoma after radiofrequency thermal ablation. *J Immunother*. 2008;31(3):271–282.
14. Johnson JD, Fleshner M. Releasing signals, secretory pathways, and immune function of endogenous extracellular heat shock protein 72. *J Leukoc Biol*. 2006;79(3):425–434.
15. Pockley AG. Heat shock proteins as regulators of the immune response. *Lancet*. 2003;362(9382):469–476.
16. Srivastava P. Interaction of heat shock proteins with peptides and antigen presenting cells: chaperoning of the innate and adaptive immune responses. *Annu Rev Immunol*. 2002;20:395–425.
17. Bhardwaj N, Dormer J, Ahmad F, et al. Heat shock protein 70 expression following hepatic radiofrequency ablation is affected by adjacent vasculature. *J Surg Res*. 2012;173(2):249–257.
18. Li Z, Menoret A, Srivastava P. Roles of heat-shock proteins in antigen presentation and cross-presentation. *Curr Opin Immunol*. 2002;14(1):45–51.
19. Liu Q, Zhai B, Yang W, et al. Abrogation of local cancer recurrence after radiofrequency ablation by dendritic cell-based hyperthermic tumor vaccine. *Mol Ther*. 2009;17(12):2049–2057.
20. Wissniowski TT, Hansler J, Neureiter D, et al. Activation of tumor-specific T lymphocytes by radio-frequency ablation of the VX2 hepatoma in rabbits. *Cancer Res*. 2003;63(19):6496–6500.
21. Sanchez-Ortiz RF, Tannir N, Ahrar K, Wood CG. Spontaneous regression of pulmonary metastases from renal cell carcinoma after radio frequency ablation of primary tumor: an in situ tumor vaccine? *J Urol*. 2003;170(1):178–179.
22. Kim H, Park BK, Kim CK. Spontaneous regression of pulmonary and adrenal metastases following percutaneous radiofrequency ablation of a recurrent renal cell carcinoma. *Korean J Radiol*. 2008;9(5):470–472.
23. Bendz H, Ruhland SC, Pandya MJ, et al. Human heat shock protein 70 enhances tumor antigen presentation through complex formation and intracellular antigen delivery without innate immune signaling. *J Biol Chem*. 2007;282(43):31688–31702.
24. Binder RJ, Blachere NE, Srivastava PK. Heat shock protein-chaperoned peptides but not free peptides introduced into the cytosol are presented efficiently by major histocompatibility complex I molecules. *J Biol Chem*. 2001;276(20):17163–17171.